

Thermal Response of Poly(*N-n*-propylacrylamide)

Daisuke ITO and Kenji KUBOTA[†]

Department of Biological and Chemical Engineering, Faculty of Engineering,
Gunma University, Kiryu, Gunma 376–8515, Japan

(Received August 4, 1998)

ABSTRACT: Thermal response of poly(*N-n*-propylacrylamide) in water and aqueous nonionic surfactant solution was studied focusing on the temperature dependence of chain dimensions by static and dynamic light scattering. Interpenetration function showed unique behavior deviating from the two-parameter theory in contrast to the case of poly(*N*-isopropylacrylamide). Poly(*N-n*-propylacrylamide) molecules may thus exhibit conformational change due to hydrophobic interaction on approaching the theta temperature.

KEY WORDS Poly(*N-n*-propylacrylamide) / Volume Phase Transition / Polymer Gel / Excluded-Volume Effect / Nonionic Surfactant / Light Scattering /

Volume phase transition is the most characteristic and interesting feature of polymeric gels.¹ This feature is related to the structure of crosslinking in the gel, interactions between the network polymer chains, and interactions between the network chain and solvent. Such a transition can be induced reversibly by various external conditions: temperature, pH, ionic strength, solvent composition, and so on.² The volume phase transition in hydrogels has been most extensively studied, and electrostatic interaction, van der Waals force, hydrogen bonding, and hydrophobic interaction are the essential interactions.³

In a recent paper on the thermal behavior of poly(*N-n*-propylacrylamide) (PN*n*PAM) in water,⁴ a very sharp decrease of chain dimensions and second virial coefficient occurs near the theta temperature, 22.54°C, and interpenetration function as a function of the expansion factor was found to deviate from the prediction of the recent two-parameter theory substantially and systematically. These features are very different from the common behavior of synthetic polymers, possibly since qualitative conformational change likely occurs due to hydrophobic interaction. This might be one of the reasons why PN*n*PAM differs from poly(*N*-isopropylacrylamide) (PNiPAM) in thermal response. Although aqueous solution of PNiPAM exhibits a clear coil-globule transition over the theta temperature, PN*n*PAM becomes unstable just above the theta temperature. NiPAM gel shows much weaker discontinuity in volume phase transition.^{5,6} NiPAM gel exhibits substantially discontinuous volume phase transition.⁷ Because NiPAM gel is a nonionic gel and electrostatic interaction does not take place, discontinuous volume phase transition should originate from the physicochemical nature of PN*n*PAM chains themselves. The chain stiffening of PN*n*PAM molecules may result from the conformational change in the consideration of chain sizes using wormlike chain model.⁴ The stiffening of PN*n*PAM chains due to the hydrophobic interaction with approach to the theta temperature is quite agreeable with the behavior of NiPAM gel, and elucidates well the difference between NiPAM gel and PNiPAM gel. It has been theoretically predicted that chain

stiffness causes discontinuous volume phase transition of polymer gels.⁸

The variation of stiffness with temperature means that the unperturbed chain dimensions far apart from the theta temperature should differ from those at the theta temperature. The Yamakawa theory for the excluded-volume effect shows that the interpenetration function is related not only to solvent conditions but also chain length (in other words, chain stiffness).^{9–11} In case of PN*n*PAM in water, both changes of solvent conditions and chain stiffness should occur simultaneously. Then, maximum behavior of interpenetration function may appear.

In our previous results, such behavior was not clear enough. Therefore, we studied the thermal behavior of PN*n*PAM molecules in the presence of nonionic surfactant, and discuss the effect of surfactant relating to the chain conformation. Nonionic surfactant was chosen to change the solvent conditions in a restricted manner.

EXPERIMENTAL

PN*n*PAM, $M_w = 1.59 \times 10^6$ and $M_w/M_n < 1.2$, was used in this study. M_w and M_n are the weight average and number average molecular weight, respectively. The characterization of molecular parameters in water at 10°C was obtained previously, and is described in detail elsewhere.⁴ Water was distilled, and obtained by Milli-Q (resistivity, 18.3 MΩ). Nonionic surfactant, octaethyleneglycol mono-*n*-dodecyl ether (C₁₂E₈), was purchased from Nikko Chem. Co. Ltd. and was used without further purification. Concentration of C₁₂E₈ was adjusted to 8 mM.

The details of the experimental setup are described in our previous paper.^{4,12} Light source was Ar ion laser operated at 488.0 nm. Zimm plots in the square-root form were used to obtain accurate second virial coefficients and radii of gyration. To compare the results for PN*n*PAM in water with the present results, the previous data of PN*n*PAM in water (sample G in ref 4) were reanalyzed using the same procedures. Correlation function measurements were carried out by an ALV-5000/E multiple-tau digital correlator. The auto-

[†] To whom correspondence should be addressed.

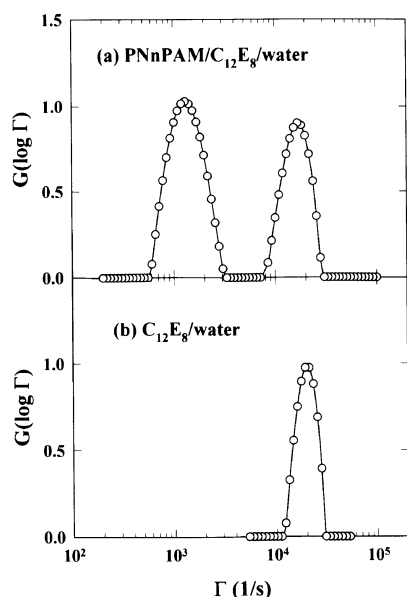


Figure 1. Decay rate distribution of poly(*N-n*-propylacrylamide) in aqueous 8 mM $C_{12}E_8$ solution ($c=0.225 \text{ mg cm}^{-3}$) (a) and aqueous 8 mM $C_{12}E_8$ solution (without PNnPAM) (b) at 9.75_8°C and $\theta=60^\circ$. The fast decay rate peak in (a) corresponds to the micellar assembly of $C_{12}E_8$ as shown in (b). Solid curves are guides to eye.

correlation function of the scattered light intensity, $G^{(2)}(\tau)$, obtained by the homodyne mode was analyzed by CONTIN method (CONTIN 2DP).¹³ The hydrodynamic radius R_h was evaluated using the Stokes–Einstein equation. Viscosity of aqueous 8 mM $C_{12}E_8$ solution was measured at various temperatures using an Ubbelohde type viscometer which was calibrated by water as a reference standard.

RESULTS AND DISCUSSION

Scattered light intensity data were analyzed using the Zimm plots in the square-root form. In case of $C_{12}E_8$ solution, surfactant molecules are possibly adsorbed on the polymer chain and the concentration of $C_{12}E_8$ in water differs from the original concentration (8 mM). Because the critical micellar concentration of $C_{12}E_8$ in water at 10°C is reported as 0.156 mM,¹⁴ spherical micelles of $C_{12}E_8$ must be formed in the solution. This was examined by correlation function measurements, and decay rate distribution of the PNnPAM solution and of the aqueous $C_{12}E_8$ solution were obtained. For PNnPAM solution in the aqueous 8 mM $C_{12}E_8$ solution, two peaks appeared in the decay rate distribution split clearly by about one order as shown in Figure 1. Decay rate distribution was obtained for various scattering angles, polymer concentrations, and temperatures. Two (fast and slow) peaks appeared in every case, and both showed q^2 -dependence indicating a diffusive mode. The decay rate of the fast mode coincides almost exactly to that of the decay rate distribution obtained for the aqueous $C_{12}E_8$ solution (without PNnPAM). The average diameter was 6–7 nm. The average decay rate of the fast mode is essentially unchanged with the change of scattering angle and polymer concentration. Since the integration of the decay rate distribution is proportional to the scattered intensity for the fraction of the integrating

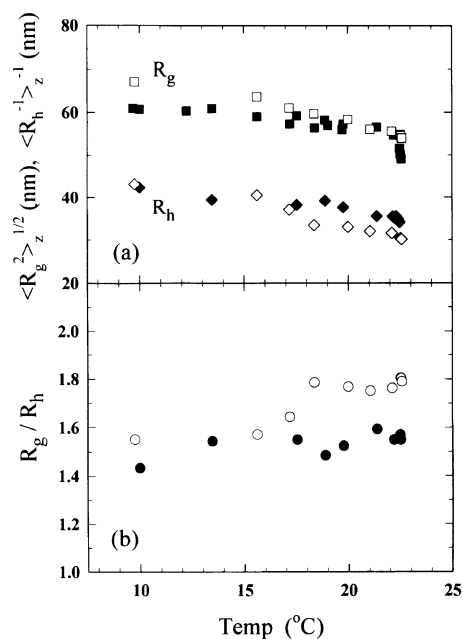


Figure 2. Temperature dependence of the radius of gyration R_g and hydrodynamic radius R_h (a) and the ratio of them R_g/R_h (b) for PNnPAM in water and in the aqueous 8 mM $C_{12}E_8$ solution. Solid and hollow symbols denote PNnPAM in water and PNnPAM in the aqueous 8 mM $C_{12}E_8$ solution, respectively.

range, the magnitude of the scattered intensity due to $C_{12}E_8$ can be evaluated from the decay rate distribution and total scattered intensity. Intensity due to $C_{12}E_8$ agrees well with that of the aqueous 8 mM $C_{12}E_8$ solution (without PNnPAM) within $\pm 3\%$ for all scattering angles, polymer concentrations, and temperature. This means that the adsorption of $C_{12}E_8$ to PNnPAM molecules is not appreciable (even if adsorption takes place, it should be very weak), and micelles of $C_{12}E_8$ behave independently of PNnPAM molecules in the present experimental conditions. The presence of $C_{12}E_8$ affects solvent quality. Therefore, excess scattered intensity of PNnPAM was obtained by subtracting the scattered intensity of the solvent (8 mM $C_{12}E_8$ aqueous solution) from that of the PNnPAM solution. The molecular weight of PNnPAM measured at 9.75_8°C was 1.64×10^6 , and the increase from that in aqueous solution (1.59×10^6) was only $\sim 3\%$. Variance of the slow peak (PNnPAM mode) at $\sim 10^\circ\text{C}$ is also almost the same as that obtained for PNnPAM in water, and increases with temperature (from ~ 0.1 at $\sim 10^\circ\text{C}$ to 0.15–0.2 near the theta temperature).

Figure 2 shows the temperature dependence of the radius of gyration R_g and hydrodynamic radius R_h in panel (a), and the ratio R_g/R_h in panel (b). The second virial coefficient became equal to zero at 22.56°C , the theta temperature, for PNnPAM in 8 mM $C_{12}E_8$ solution and showed a sharp decrease near the theta temperature. This temperature is almost the same as that of PNnPAM in water, 22.54°C . When the temperature exceeds by *ca.* 0.05°C above the theta temperature, the solution becomes unstable and the aggregations of PNnPAM molecules were formed to give an opaque solution. The solubilization of collapsed PNnPAM aggregates by the adsorption of surfactant molecules did not take place. R_g of PNnPAM in aqueous 8 mM $C_{12}E_8$ solution is sub-

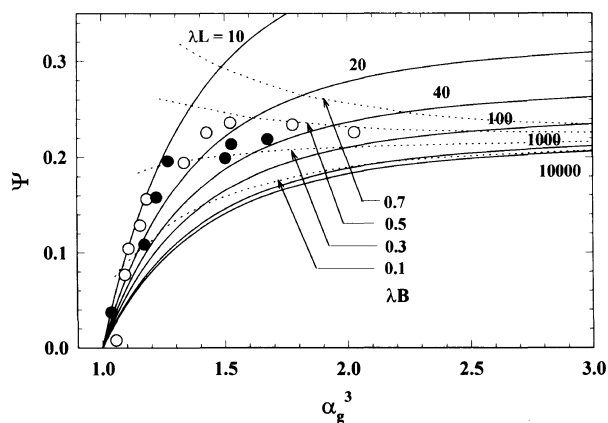


Figure 3. Relationships between interpenetration function Ψ and the expansion coefficient α_g^3 . ● stands for PNnPAM in water and ○ for PNnPAM in the aqueous 8 mM $C_{12}E_8$ solution. The solid curves are predicted curves by the two-parameter theory of Yamakawa theory and Domb–Barrett function for the expansion factor. The solid and dotted curves denote the calculated curves for fixed values of λL and λB , respectively.

stantially larger (about 10%) than that in water at about 10°C, and 4.5% larger in R_h . This implies that the addition of nonionic surfactant enlarges the chain dimensions. The temperature dependence of the radius of gyration and hydrodynamic radius of PNnPAM in 8 mM $C_{12}E_8$ are very similar to that in water. However, the temperature dependence of R_g and R_h seems not to be monotonous. A weak flexion in R_g and a substantial decrease in R_h were observed in the course of temperature increase.

The ratio of R_g to R_h shows a unique temperature dependence. Panel (b) of Figure 2 depicts the temperature dependence of R_g/R_h for PNnPAM in water and aqueous 8 mM $C_{12}E_8$ solution. R_g/R_h in water solution shows only a slight increase with approaching the theta temperature. PNnPAM in 8 mM $C_{12}E_8$ shows a significant increase. It seems that there occurs a stepwise-like increase around 18°C. This temperature corresponds to the temperature where nonmonotonous decrease of chain dimensions was observed. At lower temperature region $R_g/R_h \sim 1.5$ and at higher temperature region $R_g/R_h \sim 1.8$. This increase is not explained by the decrease of chain dimensions due to the solvent quality only, in other words by the excluded-volume effect only.

To study these points in more detail, the interpenetration function was examined as a function of the expansion factors. The interpenetration function, Ψ , is defined as¹⁵

$$\Psi = A_2 M_w^2 / 4\pi^{3/2} N_A \langle R_g^2 \rangle_z^{3/2} \quad (1)$$

where N_A is the Avogadro's number. Recent polymer solution theory based on the two-parameter theory is given by Barrett theory¹⁶ for Ψ and the Domb–Barrett equation¹⁷ for the expansion factor α_g as

$$\Psi = (z/\alpha_g^3) / (1 + 14.3z + 57.3z^2)^{0.2} \quad (2)$$

$$\alpha_g^2 = [1 + 10z + (70\pi/9 + 10/3)z^2 + 8\pi^{3/2}z^3]^{2/15} \times [0.933 + 0.067 \exp(-0.85z - 1.39z^2)] \quad (3)$$

Here, z is the familiar excluded-volume parameter and $\alpha_g^2 = \langle R_g^2 \rangle_z / \langle R_g^2 \rangle_{z,\theta}$ with $\langle R_g^2 \rangle_{z,\theta}$ being the mean square radius of gyration at the theta temperature. Figure 3

shows the interpenetration function as a function of α_g^3 together with the results of PNnPAM in water. The results of PNnPAM in water were reanalyzed as noted above. In Figure 3 theoretical curves calculated by the Yamakawa theory (quasi-two-parameter theory)^{11,18–20} are drawn for various λL and λB . The interpenetration function in this frame work is a function not only of solvent conditions, but also chain stiffness. Here, the wormlike (KP) chain model was assumed and λ is the stiffness parameter, and $(2\lambda)^{-1}$ can be approximated to the persistence length. The introduction of the chain stiffness into the frame work of the excluded-volume effect causes modification of the excluded-volume parameter by \tilde{z} instead of z and the modification of Barrett function by \tilde{z} instead of z , as $\tilde{z} = (3/4)K(\lambda L)z$ and $\tilde{z} = (Q/2.865)(z/\alpha_g^3)$. $K(\lambda L)$ and Q have been given by Yamakawa.¹¹ The effects of chain ends were neglected in the present calculation. The solid curve shows the interpenetration function by change of solvent condition, λB , for a fixed λL . B is excluded-volume strength which expresses interactions between chain segments. The interpenetration function for fixed solvent conditions is illustrated by dotted curves. From the theoretical curves, it is expected that the interpenetration function increases with decrease of λL and λB and with a larger decrease of λL than that of λB at some conditions and shows a maximum, although such a maximum behavior should be a weak one.^{10,21}

For the interpenetration function of PNnPAM in water, maximum behavior is not so clear and the variation of it is rather monotonous. The interpenetration function of PNnPAM in aqueous 8 mM $C_{12}E_8$ solution shows a maximum around $\alpha_g^3 \sim 1.5$ (although a weak one) and intersects with the theoretical curves clearly. The temperature for this maximum corresponds to the region of nonmonotonous behavior of chain dimensions and stepwise-like increase of R_g/R_h . Thus, λL of PNnPAM chain changes with temperature, and supports that the shrinkage of PNnPAM chain does not proceed uniformly but a conformational change occurs simultaneously. It should be pointed out that α_g^2 far apart from the theta temperature might be underestimated, because the unperturbed radius of gyration could be smaller than the value obtained at the temperature for $A_2 = 0$. For example, α_g^2 at 9.75°C could be about 5 and datapoint at that temperature might correspond to $\lambda L \sim 1000$. This estimation is quite reasonable for a rough evaluation of the persistence length of about 1.2 nm, and the excluded-volume effect should be effective there. In fact, using the same values of contour length, diameter, and persistence length of the wormlike chain model as those used for PNnPAM in water (3500, 1.5, and 1.2 nm, respectively, see ref 4) and $\lambda B = 0.34$, R_g and R_h are calculated as 67.2 and 41.6 nm for $M_w/M_n = 1.2$, respectively. The agreement with the experimental results, 67.1 and 43.2 nm, is good. For aqueous solution, $\lambda B = 0.26$ was estimated. These combinations give good agreement with the experimental R_g , R_h , and $[\eta]$ of PNnPAM in water at 10°C, and are reasonable for usual vinyl polymers.⁴ The increase of λB parallels the increase of chain dimensions and A_2 at $\sim 10^\circ\text{C}$ for PNnPAM in aqueous 8 mM $C_{12}E_8$ solution. However, the calculated R_g and R_h by the same parameter values for the values

APPENDIX

at the theta temperature are underestimated very much compared with the experimental ones: 34% in R_g (experimental value is 54.0 nm and calculated value is 40.4 nm) and 20% in R_h (experimental value is 30.1 nm and calculated value is 25.1 nm). Such underestimation has been observed in PN*n*PAM in water. This underestimation suggests that the values (contour length, diameter, and persistence length) of wormlike chain model should change in the course of temperature increase in agreement with the occurrence of conformational change. That PN*n*PAM molecules form local clustering, which should proceed nonuniformly, is consistent with the increase of variance of PN*n*PAM peak in the decay rate distribution when approaching the theta temperature. The linear structure of hydrophobic *n*-propyl group favors the clustering. The clustering might cause decrease of contour length of PN*n*PAM molecules and effective increase of chain stiffness by the steric hindrance. The simultaneous decrease of λL with the decrease of solvent condition is agreeable with the behavior of chain dimensions and R_g/R_h . Because of the cancellation of the decrease of contour length and increase of effective chain stiffness, only a weak change appears in the temperature dependence of chain dimensions. The ratio R_g/R_h reflects such a change more clearly. For example, the combination of the contour length = 1000 nm, diameter = 6 nm, and persistence length = 7 nm assuming Schulz Zimm distribution for the molecular weight distribution ($M_w/M_n \sim 1.2$) gives $R_{g,\theta} = 51.7$ and $R_{h,\theta} = 32.7$ nm at the theta temperature. These values are more reasonable compared with the experimental values at the theta temperature (54.0 and 30.1 nm, respectively). The magnitude of the persistence length of 7 nm is a little larger than that used for PN*n*PAM in water.⁴ These values are very rough and are not definite. Quantitative evaluation is still difficult. It should be mentioned here that we did not analyze at the present the effects of torsional rigidity by the helical wormlike chain model because of the complexity of theoretical treatment. Such an effect may result from the conformational change contributes more or less.

In conclusion, temperature dependence of the chain dimensions of PN*n*PAM in water and an aqueous 8 mM C₁₂E₈ solution was examined. The change of chain dimension with the temperature is not uniform and conformational change, clustering of the chain, occurs in the temperature region substantially below the theta temperature due to hydrophobic interaction. This conformational change may be accompanied with decrease of contour length and increase of effective chain stiffness, although quantitative evaluation is difficult at the present stage. These features were enhanced by the addition of nonionic surfactant compared to that of PN*n*PAM in water.

Acknowledgments. We are thankful for the grant-in-aid from the Ministry of Education, Science, Sports and Culture of Japan.

The scheme that PN*n*PAM molecules exhibit a conformational change preceding the theta temperature (around at 18°C) was further examined using 1-anilinonaphthalene-8-sulfonate (ANS) as a fluorescent probe. ANS was added to make 10 μM L⁻¹ in an aqueous solution of 0.1 mg cm⁻³ of the present PN*n*PAM sample, and the emission spectrum excited by 350 nm line was monitored as a function of temperature. ANS was chosen because ANS characterizes microscopic circumstances around dye molecules. The maximum wavelength of emission spectra $\lambda_{EM,max}$ decreases (blue shift) and the fluorescence quantum yield increases with hydrophobicity. Clear change of $\lambda_{EM,max}$ (decrease) and emitted light intensity (increase) was observed in the temperature region starting at ~18°C even in this very dilute solution, where scattered light does not increase. The solution may thus be stable in this temperature range. The increase of hydrophobic interaction substantially below the transition temperature (~theta temperature) agrees well with conformational change where local clustering of *n*-propyl groups traps ANS molecules firmly in a hydrophobic field. A clearer confirmation of conformational change can be obtained by the analyses of fluorescence spectrum using fluorescent dye probe covalently bonded to PN*n*PAM chains directly, *e.g.*, peak wavelength of emission spectra, emission anisotropy, and rotational diffusion coefficient of fluorescent group. Such study is in progress.

REFERENCES

1. T. Tanaka, *Phys. Rev. Lett.*, **40**, 820 (1978).
2. A. Suzuki and T. Tanaka, *Nature*, **346**, 345 (1990).
3. T. Tanaka, M. Annaka, K. Ilmain, E. Ishii, E. Kokufuta, A. Suzuki, and M. Tokita, *NATO ASI Ser.*, **H64**, 683 (1992).
4. D. Ito and K. Kubota, *Macromolecules*, **30**, 7828 (1997).
5. K. Kubota, S. Fujishige, and I. Ando, *J. Phys. Chem.*, **94**, 5154 (1990).
6. C. Wu and S. Zhou, *Macromolecules*, **28**, 8381 (1995).
7. H. Kawasaki, T. Nakamura, K. Miyamoto, M. Tokita, and T. Komai, *J. Chem. Phys.*, **103**, 6241 (1995).
8. T. Tanaka, D. J. Fillmore, S.-T. Sun, I. Nishio, G. Swislow, and A. Shah, *Phys. Rev. Lett.*, **45**, 1636 (1980).
9. H. Yamakawa, F. Abe, and Y. Einaga, *Macromolecules*, **26**, 1898 (1993).
10. T. Arai, N. Sawatari, T. Yoshizaki, Y. Einaga, and H. Yamakawa, *Macromolecules*, **29**, 2309 (1996).
11. H. Yamakawa, *Macromolecules*, **25**, 1912 (1992).
12. K. Kubota, H. Urabe, Y. Tominaga, and S. Fujime, *Macromolecules*, **17**, 2096 (1984).
13. S. W. Provencher, *Computer Phys. Comm.*, **27**, 213 (1982).
14. M. J. Rosen, A. W. Cohen, M. Dahanayake, and X. Y. Hua, *J. Phys. Chem.*, **86**, 541 (1982).
15. H. Yamakawa, "Modern Theory of Polymer Solution," Harper & Row, New York, N.Y., 1971.
16. A. J. Barrett, *Macromolecules*, **18**, 196 (1985).
17. C. Domb and A. J. Barrett, *Polymer*, **17**, 179 (1976).
18. H. Yamakawa and W. H. Stockmayer, *J. Chem. Phys.*, **57**, 2843 (1972).
19. H. Yamakawa and J. Shimada, *J. Chem. Phys.*, **83**, 2607 (1985).
20. J. Shimada and H. Yamakawa, *J. Chem. Phys.*, **85**, 591 (1986).
21. F. Abe, Y. Einaga, and H. Yamakawa, *Macromolecules*, **27**, 3262 (1994).